

Colossal non-saturating linear magnetoresistance in two-dimensional electron systems at a GaAs/AlGaAs heterointerface

M. A. Aamir,^{1,*} Srijit Goswami,¹ Matthias Baenninger,² Vikram Tripathi,³
Michael Pepper,⁴ Ian Farrer,² David A. Ritchie,² and Arindam Ghosh¹

¹*Department of Physics, Indian Institute of Science, Bangalore 560 012, India.*

²*Cavendish Laboratory, University of Cambridge,*

J.J. Thomson Avenue, Cambridge CB3 0HE, United Kingdom.

³*Department of Theoretical Physics, Tata Institute of Fundamental Research, Homi Bhabha Road, Mumbai 400005, India*

⁴*Department of Electrical and Electronic Engineering,
University College, London WC1E 7JE, United Kingdom*

Engineering devices with a large electrical response to magnetic field is of fundamental importance for a range of applications such as magnetic field sensing and magnetic read-heads. We show that a colossal non-saturating linear magnetoresistance (NLMR) arises in two-dimensional electron systems hosted in a GaAs/AlGaAs heterostructure in the strongly insulating regime. When operated at high source-drain bias, the magnetoresistance of our devices increases almost linearly with magnetic field reaching nearly 10,000% at 8 Tesla, thus surpassing many known non-magnetic materials that exhibit giant NLMR. The temperature dependence and mobility analysis indicate that the NLMR has a purely classical origin, driven by nanoscale inhomogeneities. A large NLMR combined with small device dimensions makes these systems a new and attractive candidate for on-chip magnetic field sensing.

In a non-magnetic semiconductor, giant positive linear non-saturating magnetoresistance (NLMR) can have both classical [1–4] and quantum origin [5, 6]. The quantum NLMR, originally proposed by Abrikosov [5, 6], is applicable in the extreme quantum limit where $\hbar\omega_c \gg E_F, k_B T$ (ω_c and E_F are the cyclotron frequency and Fermi energy, respectively). This criterion can be attained in a restricted class of materials which include semimetals such as bismuth, or narrow band gap semiconductors with very low effective mass (*e.g.* InSb [3], graphene [7], and topological insulators [8]). The classical NLMR, on the other hand, is commonly observed in systems with an inhomogeneous carrier (and hence mobility) distribution [4, 9]. It is a purely geometric effect, where, in the presence of transverse magnetic field, a misalignment between current paths and the externally applied bias mixes the off-diagonal components of the magnetoresistivity tensor, resulting in a NLMR. Several classically inhomogeneous conductors, most notably the mildly doped silver chalcogenides ($\text{Ag}_{2+\delta}\text{Se}$ or $\text{Ag}_{2+\delta}\text{Te}$) [1] and InSb polycrystals [3], display extremely large NLMR, where the inhomogeneity is associated with intrinsic disorder such as grain boundaries, dopant clustering etc. Thus a handle on the disorder, both in magnitude and length scale, could yield a new class of high sensitivity magnetoresistive devices. However, achieving such a control in bulk materials is not a trivial task.

Two-dimensional electron systems (2DESs) in semiconductor multi-layers, in particular doped GaAs/AlGaAs heterostructures, offer a material platform in which disorder can be tuned with great precision using molecular beam epitaxy. At high carrier density, since the hetero-interface is physically separated from the ionized dopants, it is a homogeneous medium

which hosts high mobility electrons. Therefore, it is not expected to be a good candidate for exhibiting NLMR. This is confirmed by numerous magnetoresistance (MR) measurements in 2DES, which are best studied in two limits. At high carriers densities, the MR of a 2DES is oscillatory in magnetic field (B) due to the Shubnikov-de Haas effect, while at lower carrier densities, at the onset of localization, the MR increases exponentially with B due to variable range hopping [10]. Clearly, studies in neither regime have thus far revealed a NLMR.

A 2DES however does become inhomogeneous when it is depleted with a strong negative gate voltage (V_g) [11]. This constitutes the backbone of our experiments in the following way: for a typical doped GaAs/AlGaAs heterostructure with spacer thickness d , the Coulomb potential from the randomly scattered ionized dopants form the dominant component of disorder. This causes the conduction band minimum to fluctuate as a function of position (see Fig. 1b) with a correlation length of $\sim 2d$ [12–14]. In this regime, the 2DES disintegrates into small puddles of charge that often manifest in Coulomb blockade effects in mesoscopic devices [11, 13, 15]. In essence, this increase in inhomogeneity arises due to the weakening of electrostatic screening of the background disorder potential landscape, causing the spatial fluctuations in carrier density to be of the same order as the carrier density itself. We show that such a strong density variation at the GaAs/AlGaAs interface does in fact give rise to a giant NLMR in a simple gate-tunable mesoscopic system.

Our experiments are carried out in strongly insulating 2DES's in the GaAs/AlGaAs heterostructure where we explore the magnetic response of the system as a function of gate voltage (V_g) and drain-source bias (V_{sd}). The

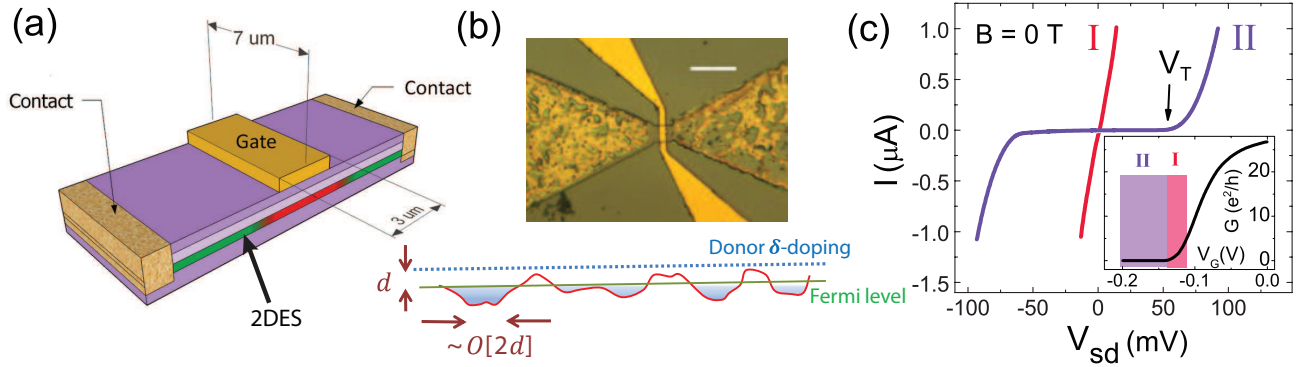


FIG. 1: (a) Schematic of the device — the gate modulates the electron number density only in region of 2DES below it (highlighted red) thus defining the mesoscopic region of interest (b) Top: Optical micrograph of the device. Scale bar is $20 \mu\text{m}$. Bottom: Potential landscape profile for the electrons at very low number density (c) Inset: Equilibrium conductance as a function of the gate voltage. Region I represents gate voltage just above the pinch-off (the point when equilibrium conductance becomes zero); Region II represents another set of gate voltages below the pinch-off point. The main figure shows $I - V$ characteristics of the device for these two distinct regions at 0.3 K. The arrow indicates the threshold voltage V_T .

heterostructures contain a δ -doped layer of Si dopants of doping density $2.5 \times 10^{12} \text{ cm}^{-2}$ placed 40 nm above the GaAs/AlGaAs interface. The 2DES lies 90 nm below the

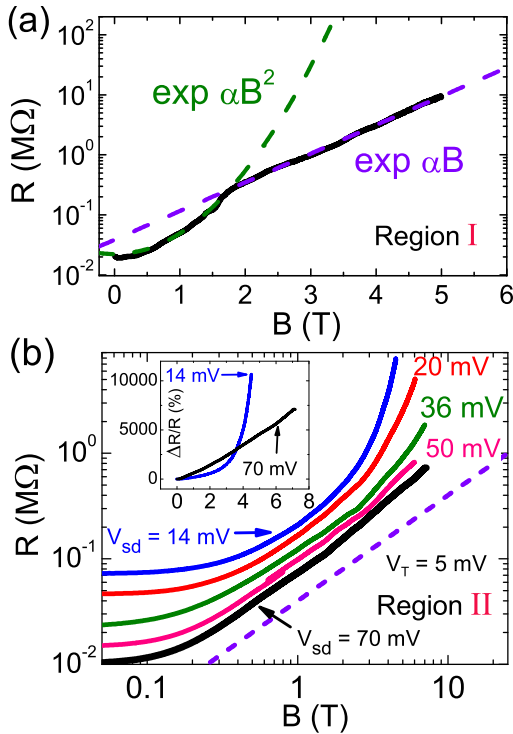


FIG. 2: (a) MR of the sample for gate voltages above the pinch-off voltage (Region I) obtained using ac lock-in measurements (b) MR at different V_{sd} below the pinch-off point (Region II). As source-drain is increased, the MR gradually transforms from a rapidly rising curve to a power law with exponent 1.1. The dashed line is $R \propto B$. Inset: Percentage change in resistance $\Delta R/R$ (%) for two V_{sd} of 14 mV and 70 mV

surface, with an as-grown mobility $\sim 300 \text{ m}^2/\text{Vs}$. The etched mesa and a surface gate define the effective geometry of the device. Here we present results from a $3 \mu\text{m} \times 7 \mu\text{m}$ device (see Fig. 1a and Fig. 1b), though similar devices on two separate wafers showed qualitatively similar results (see Supplementary Material). The gate is used to pinch the device off by application of a negative voltage, and the resulting conductance curve is shown in the inset of Fig. 1c. Fig. 1c shows $I - V_{sd}$ characteristics at two values of V_g , representative of the two regions identified as Regions I and II. Region I represents the onset of localization at linear conductance $G \sim e^2/h$, and has a reasonably ohmic $I - V_{sd}$. Region II however lies deep in the pinched-off regime where the 2DES is expected to become inhomogeneous. Here, we find the $I - V_{sd}$ characteristics are strongly non-linear with an insulating regime up to a threshold voltage V_T (indicated by an arrow in Fig. 1c), which increases monotonically as V_g is made increasingly negative (see Supplementary Material). Within this threshold, the current is immeasurably small ($< 10^{-11} \text{ A}$), and conduction sets in rapidly only after the source-drain bias is increased beyond V_T . This rapid rise of current above threshold cannot be associated with avalanche breakdown common in semiconductors [16–18]. This is because the applied electric fields are 3 orders of magnitude lower than the breakdown field in GaAs [17]. The strong dependence of $I - V_{sd}$ curves on magnetic field (to be discussed later) also eliminates self-heating effects as a cause for the rapidly rising current. In fact, a systematic analysis of the $I - V_{sd}$ characteristics reveals that they follow a power law, characteristic of a disordered array of charge puddles (see Supplementary Material). This provides direct evidence that in Region II the system is indeed highly inhomogeneous.

This inhomogeneity has a dramatic effect on the MR when subjected to a transverse magnetic field. At the

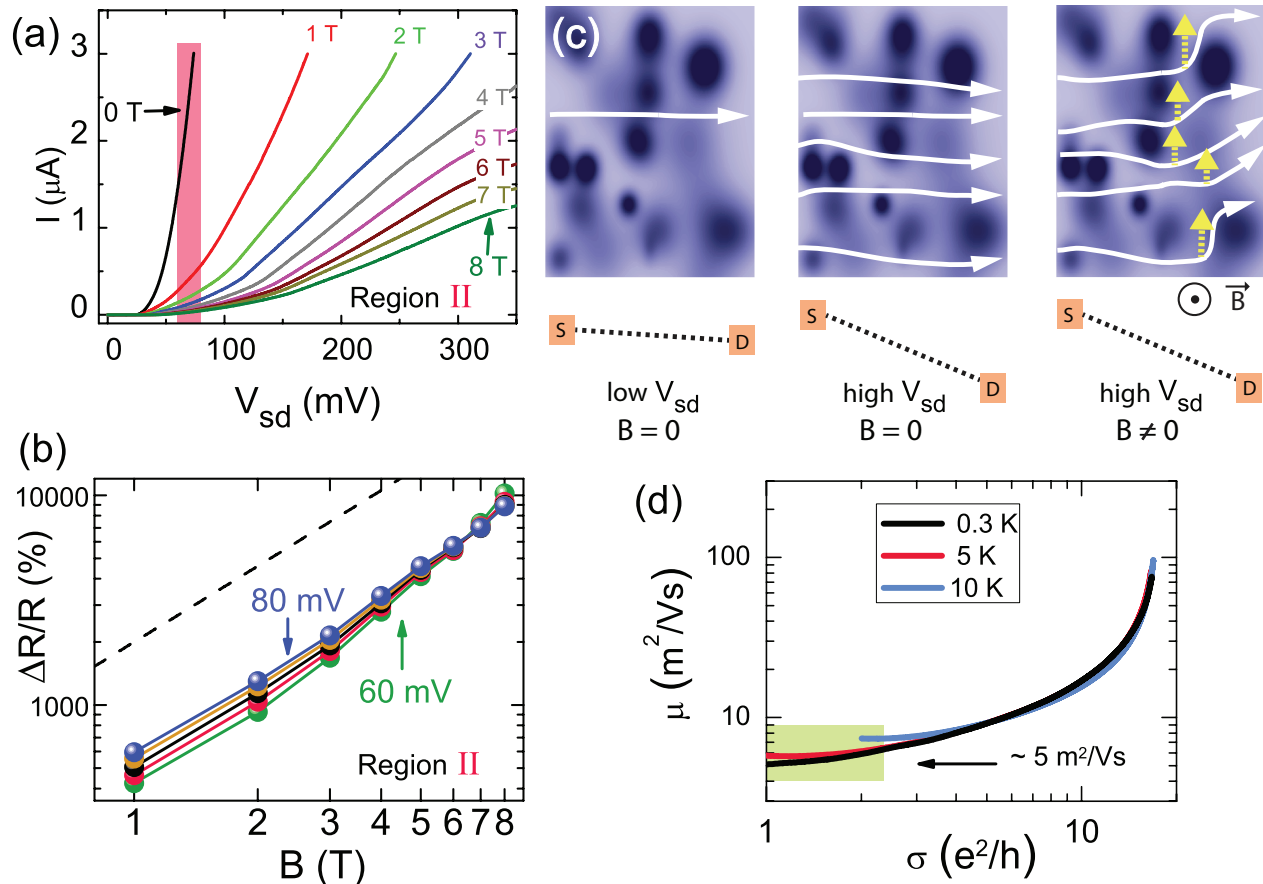


FIG. 3: (a) $I - V_{sd}$ characteristics as a function of magnetic field from 0 T to 8 T (in steps of 1 T) at 0.3 K (Region II) (b) $\Delta R/R$ (%) for different V_{sd} chosen from the shaded region of (a) (V_{sd} step size is 5 mV) (c) A schematic illustrating the possible origin of NLMR: The light (dark) regions represent areas of high (low) carrier number density. White arrows represent the current paths. Left: At low V_{sd} , there is only one or very few current channels. Middle: For high V_{sd} , the number of current paths proliferate rapidly. Right: On applying a perpendicular magnetic field at high V_{sd} , the plurality of the paths in the disordered medium gives rise to non-trivial current trajectories which have significant transverse component (highlighted by dotted yellow arrows) that mixes the Hall contribution into the longitudinal MR, thus giving rise to NLMR (d) The mobility (calculated using Drude's formula) as a function of the conductivity of the device at 0.3 K, 5 K and 10 K.

onset of localization (prior to pinch-off), represented by Region I in Fig. 1c, the resistance R (obtained using equilibrium measurements) increases exponentially with B . As shown in Fig. 2a, $R \sim \exp(B^2)$ at low B , which changes to $R \sim \exp(B)$ as B exceeds 2 T. These are characteristic features of hopping transport in the perturbative (low- B) and non-perturbative (high- B) regime, and recently studied in detail by some of us [10]. In the sub pinch-off regime, represented by Region II, R was found to behave very differently. Most notably, its structure is highly sensitive to the magnitude of V_{sd} . To elucidate this, we define the dc magnetoresistance $R = R(V_{sd}, B) = V_{sd}/I(V_{sd}, B)$, and plot it as a function of B for different values of V_{sd} in Fig. 2b (we carried out the same analysis with differential resistance $dV_{sd}/dI(V_{sd}, B)$, which did not yield significantly dif-

ferent result). Strikingly, the variation in R weakens with increasing V_{sd} , and for sufficiently high $V_{sd} \gg V_T$ ($V_T \approx 5$ mV at $V_g = -0.174$ V, $B = 0$ T), R increases linearly with B . In order to quantify the change in R , we evaluate the percentage change

$$\frac{\Delta R}{R} (\%) = \frac{[R(V_{sd}, B) - R(V_{sd}, 0)]}{R(V_{sd}, 0)} \times 100\%$$

This quantity has been plotted for the two extremal V_{sd} in the inset of Fig. 2b, which clearly shows that even the percentage change in R has transformed from a rapidly rising exponential curve to a strikingly linear form.

To study this more systematically, we look at the evolution of the $I - V_{sd}$ characteristics as B is increased from 0 to 8 T. We have chosen a gate voltage corresponding to $V_T \approx 30$ mV (see Supplementary Material). Fig. 3a

shows that a non-zero B suppresses the current drastically, leading to a positive MR that increases monotonically with B . Within the experimentally achievable B (8 T) the measured R did not show any sign of saturation. We have evaluated $\Delta R/R$ (%) (as defined above) for a few values of V_{sd} above V_T (the range is highlighted in Fig. 3a). As shown in Fig. 3b, the MR in our mesoscopic 2DES reaches almost 10,000% at $B = 8$ T for $V_{sd} = 80$ mV. As expected from Fig. 2b, the MR becomes nearly linear with increasing V_{sd} . The dashed line in Fig. 3b represents $\Delta R/R \propto B^{1.2}$.

The inherent inhomogeneity in charge distributions and a parabolic dispersion relation for the carriers makes the classical model for NLMR proposed by Parish and Littlewood [4, 9] particularly applicable in our devices. The findings in Ref. 4 followed from a numerical simulation of an equivalent node-link network model. Using the same physical principles, we have presented in the Supplementary Material an alternate theoretical analysis for NLMR in an inhomogeneous conductor, which augments existing theoretical descriptions [4, 9, 19–22]. The classical model requires current flow from source to drain to occur via multiple channels in order to realize the non-trivial magnetic response of NLMR. The process by which NLMR arises in our devices is depicted schematically in Fig. 3c. At low V_{sd} (left schematic), there are very few electron channels for conduction which are not sufficient in number to give rise to NLMR. However, a high V_{sd} (middle schematic) opens up many more conduction channels. This is similar to the non-equilibrium transport in disordered array of quantum dots where multiplication of paths is directly connected to the conduction threshold [23]. A perpendicular magnetic field distorts these current paths, which follows non-trivial trajectories through the inhomogeneous medium [4], resulting in a substantial transverse component (dotted arrows in right schematic). This allows a significant mixing of the off-diagonal components in the magnetoresistivity tensor, thus leading to the NLMR. This qualitative picture allows us to intuitively understand why we observe NLMR only at high values of V_{sd} . We note that studies on mildly doped Si also reported a seemingly similar dependence of the quantity $\Delta R/R$ on source-drain bias [2]. However, the NLMR there was connected to an inhomogeneous electric field in the presence of space-charge injection. This scenario is certainly not applicable in our case since the bias applied in our experiments is significantly lower than that required to induce bulk semiconductor transport [17, 18].

An important question that must be addressed is whether the inhomogeneity in our systems can quantitatively explain the magnitude and field scales associated with the observed NLMR. Being a δ -doped heterostructure, the dopant atoms are located at roughly the same distance from the 2DES, and hence the amplitude of conduction band fluctuations is unlikely to vary widely from

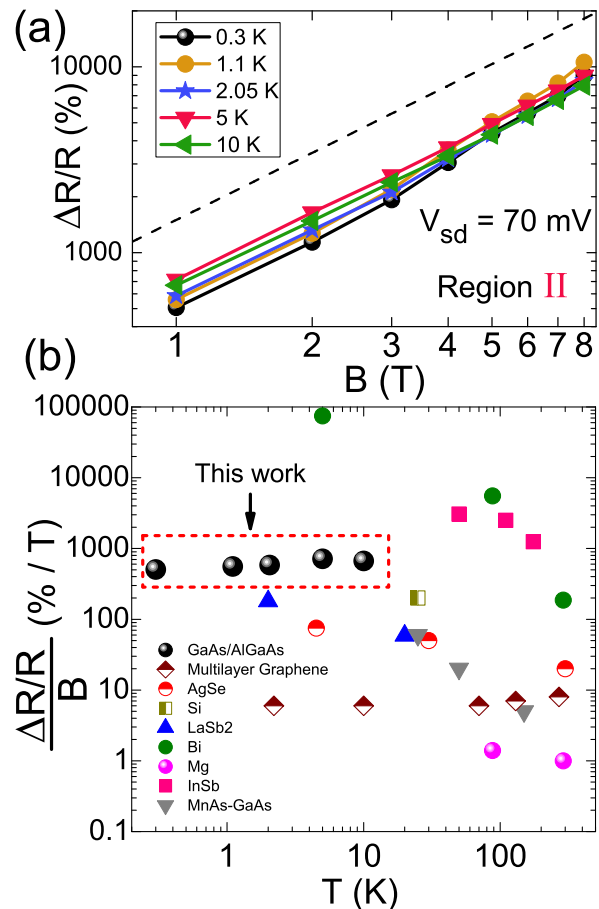


FIG. 4: (a) $\Delta R/R$ at different temperatures: 0.3 K, 1.1 K, 2.05 K, 5 K, 10 K for Region II. Dashed line represents $\Delta R/R \propto B^{1.2}$ (b) Comparison of MR of our device (highlighted by dashed box) with other non-magnetic materials which have linear MR: Ag_{2+ δ} Se [1], Multilayer graphene [7], Bulk Si [2], InSb [3], LaSb₂ [24], Bi [25, 26], Mg [27], MnAs-GaAs composite [28].

one location to another. Therefore, it is not unreasonable to assume that the width of mobility distribution $\Delta\mu$ is smaller than the average mobility $\langle\mu\rangle$ among the charge puddles. In such a case, the classical model predicts a quadratic to linear MR transition at $B \sim \langle\mu\rangle^{-1}$, with $\Delta R(B)/R = c\langle\mu\rangle B$ in the linear regime [22] (c is a constant of order unity that depends on the details of mobility distribution). From Fig. 3(b), we find that $\Delta R(B)/R(0)B \approx 5 \text{ T}^{-1}$, which is consistent with the fact that the transition to linear MR occurs around 0.1–0.2 T (see Fig 2b). Moreover, a rough estimate of $\langle\mu\rangle$ can be obtained from the mobility of the device at the onset of localization which is usually identified by conductivity $\rightarrow e^2/h$ for a 2DES. Below this conductivity, the system starts becoming disintegrated and incompressible [29]. In Fig. 3d we have shown the variation in the Drude mobility of our device as a function of its conductivity for a few temperatures. The limiting mobility at the on-

set of localization is about $5 \text{ m}^2/Vs$, which is in good order-of-magnitude agreement with $\Delta R(B)/R(0)B$. Interestingly, $\langle \mu \rangle$ is not a strong function of temperature in our heterostructures at least upto 10 K, presumably because electron-phonon interactions contribute less to the resistivity than elastic residual scattering. This should also carry over to a weak temperature dependence of the NLMR. Fig. 4a shows that, indeed, the NLMR retains roughly the same magnitude for a temperature range from 0.3 K to 10 K, thus spanning nearly two orders of magnitude.

Finally, we compare the sensitivity of the disordered GaAs/AlGaAs heterostructure with other non-magnetic systems that exhibit NLMR. The sensitivity of our device is extracted from its value at 1 T in Fig. 4a and is an increasing function of V_{sd} (see Supplementary Material). The highest value of which that is directly observed is about 500% per Tesla at $V_{sd} = 70 \text{ mV}$. In Fig. 4b we have compiled the reported values of $\Delta R(B)/R(0)B$ (in percentage per Tesla) from a wide variety of non-magnetic semiconductors and semimetals. Clearly, the sensitivity of the GaAs/AlGaAs system is comparable to existing non-magnetic materials. This, along with electrical tunability NLMR makes mesoscopic GaAs/AlGaAs heterostructures unique in comparison to other materials. In fact, more efficient and clever gating assemblies could possibly achieve an even higher sensitivity and form a new class of magnetoresistive sensors.

We would like to acknowledge support from Department of Science and Technology, Government of India and UKIERI. S.G. thanks the IISc Centenary Postdoctoral Fellowship. We are grateful to V. Venkataraman, Nigel Cooper and Peter Littlewood for useful discussions.

* Electronic address: aamir@physics.iisc.ernet.in

- [1] R. Xu, A. Husmann, T. F. Rosenbaum, M. Saboungi, J. E. Enderby, and P. B. Littlewood, *Nature* **390**, 57 (1997).
- [2] M. P. Delmo, S. Yamamoto, S. Kasai, T. Ono, and K. Kobayashi, *Nature* **457**, 1112 (2009).
- [3] J. Hu and T. Rosenbaum, *Nature Mater.* **7**, 697 (2008).
- [4] M. M. Parish and P. B. Littlewood, *Nature* **58**, 162 (2003).
- [5] A. A. Abrikosov, *Phys. Rev. B* **58**, 2788 (1998).
- [6] A. A. Abrikosov, *Phys. Rev. B* **60**, 4231 (1999).
- [7] A. L. Friedman, J. L. Tedesco, P. M. Campbell, J. C. Culbertson, E. Aifer, F. K. Perkins, R. L. Myers-Ward, J. K. Hite, C. R. Eddy, G. G. Jernigan, et al., *Nano Lett.* **10**, 3962 (2010).
- [8] H. He, B. Li, H. Liu, X. Guo, Z. Wang, M. Xie, and J. Wang, *Appl. Phys. Lett.* **100**, 032105 (pages 3) (2012).
- [9] M. M. Parish and P. B. Littlewood, *Phys. Rev. B* **72**, 094417 (2005).
- [10] M. Baenninger, A. Ghosh, M. Pepper, H. E. Beere, I. Farrer, P. Atkinson, and D. A. Ritchie, *Phys. Rev. B* **72**, 241311 (2005).
- [11] A. A. M. Staring, H. van Houten, C. W. J. Beenakker, and C. T. Foxon, *Phys. Rev. B* **45**, 9222 (1992).
- [12] V. Tripathi and M. P. Kennett, *Phys. Rev. B* **74**, 195334 (2006).
- [13] V. Tripathi and M. P. Kennett, *Phys. Rev. B* **76**, 115321 (2007).
- [14] D. Neilson and A. R. Hamilton, *Phys. Rev. B* **82**, 035310 (2010).
- [15] A. Ghosh, M. Pepper, H. E. Beere, and D. A. Ritchie, *J. Phys.: Condens. Matter* **16**, 3623 (2004).
- [16] J. J. H. M. Schoonus, F. L. Bloom, W. Wagemans, H. J. M. Swagten, and B. Koopmans, *Phys. Rev. Lett.* **100**, 127202 (2008).
- [17] Z. G. Sun, M. Mizuguchi, T. Manago, and H. Akinaga, *Appl. Phys. Lett.* **85**, 5643 (2004).
- [18] C. Ciccarelli, B. G. Park, S. Ogawa, A. J. Ferguson, and J. Wunderlich, *Appl. Phys. Lett.* **97**, 082106 (pages 3) (2010).
- [19] C. Herring, *J. Appl. Phys.* **31**, 1939 (1960).
- [20] D. J. Bergman and D. G. Stroud, *Phys. Rev. B* **62**, 6603 (2000).
- [21] D. Stroud and F. P. Pan, *Phys. Rev. B* **13**, 1434 (1976).
- [22] V. Guttal and D. Stroud, *Phys. Rev. B* **71**, 201304 (2005).
- [23] A. A. Middleton and N. S. Wingreen, *Phys. Rev. Lett.* **71**, 3198 (1993).
- [24] S. L. Bud'ko, P. C. Canfield, C. H. Mielke, and A. H. Lacerda, *Phys. Rev. B* **57**, 13624 (1998).
- [25] P. Kapitza, *Proc. Roy. Soc. London Ser. A* **119**, 358 (1928).
- [26] F. Y. Yang, K. Liu, K. Hong, D. H. Reich, P. C. Searson, and C. L. Chien, *Science* **284**, 1335 (1999).
- [27] P. Kapitza, *Proc. Roy. Soc. London Ser. A* **123**, 292 (1929).
- [28] H. G. Johnson, S. P. Bennett, R. Barua, L. H. Lewis, and D. Heiman, *Phys. Rev. B* **82**, 085202 (2010).
- [29] Y. Meir, *Phys. Rev. Lett.* **83**, 3506 (1999).

Supplementary material: Colossal non-saturating linear magnetoresistance in two-dimensional electron systems at a GaAs/AlGaAs heterointerface

M. A. Aamir,^{1,*} Srijit Goswami,¹ Matthias Baenninger,² Vikram Tripathi,³ Michael Pepper,⁴ Ian Farrer,² David A. Ritchie,² and Arindam Ghosh¹

¹Department of Physics, Indian Institute of Science, Bangalore 560 012, India.

²Cavendish Laboratory, University of Cambridge,

J.J. Thomson Avenue, Cambridge CB3 0HE, United Kingdom.

³Department of Theoretical Physics, Tata Institute of Fundamental Research, Homi Bhabha Road, Mumbai 400005, India

⁴Department of Electrical and Electronic Engineering, University College, London WC1E 7JE, United Kingdom

ANALYSIS OF THE $I - V_{sd}$ CHARACTERISTICS

Fig. 1a shows the gate voltage dependence of the $I - V_{sd}$ characteristics in Region II (as defined in the main text) at about 8 K. As is clear, the threshold V_T , which emerges in the $I - V_{sd}$ characteristics in the region II, has a distinct gate voltage dependence (Fig. 1b). This is a remarkably linear dependence which does not break down up to the lowest gate voltages that we have applied. This linear dependence was also observed in other devices in a different wafer (not shown). The voltage threshold seems to be associated with the Coulomb blockade of the puddles of electrons, which is expected to form at such negative gate voltages. It is not clear how the linear dependence emerges, but may be the outcome the manner in which gate voltage changes the voltage barrier between these puddles of electrons.

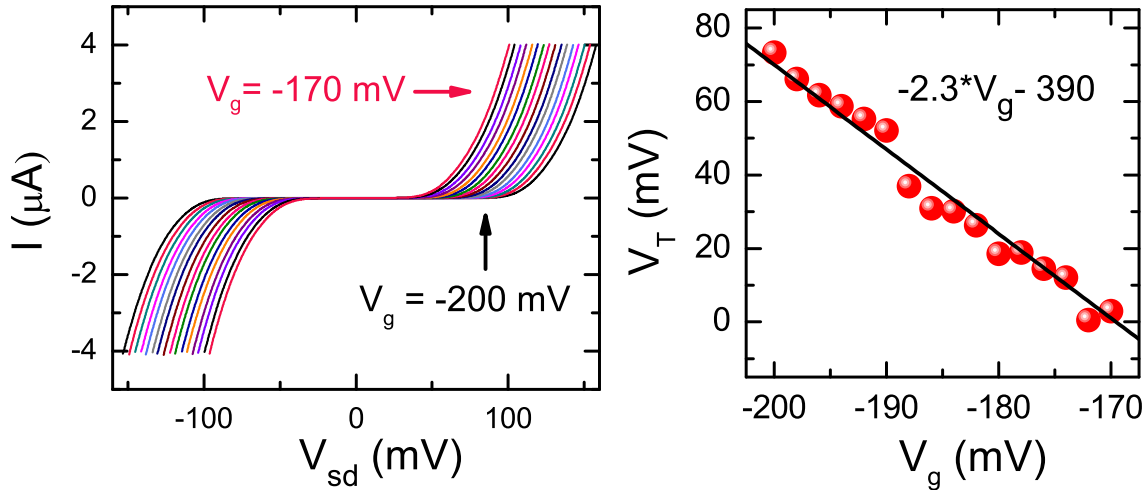


FIG. 1: (a) Gate voltage dependence of the $I - V_{sd}$ characteristics of the device in Region II from $V_g = -170 \text{ mV}$ to $V_g = -200 \text{ mV}$ in steps of 2 mV (b) Threshold voltage V_T as a function of gate voltage extracted from the $I - V_{sd}$ characteristics in (a)

The fact that the system under study is highly inhomogeneous can be further ascertained by analysing the non-linear nature of $I - V_{sd}$ characteristics. In a typical $I - V_{sd}$ curve, the current rises rapidly after having crossed the threshold V_T . The $I - V_{sd}$ characteristics, in fact, display a power law with the form $I = A(V_{sd} - V_T)^\zeta$. Fig. 2a shows this for a few magnetic fields, at 4.9 K. Interestingly, very similar $I - V_{sd}$ curves have been observed in a disordered array of quantum dots [1–7]. There, the bias threshold is directly related to the Coulomb gap of the series of quantum dots that define the electron trajectories from one lead to the other. ζ depends on the type and strength of disorder, as well as the geometry of the device. It is not surprising that such $I - V_{sd}$ curves appear in our devices as well, since the 2DES is also expected to form a disordered array of electron puddles in the pinched-off regime at very negative gate voltages [8–10].

Interestingly, the value of ζ drops sharply on the application of the magnetic field (Fig. 2b). At zero field, $\zeta = 2.8$, and falls to $\zeta = 1.8$ by 1 T and saturates thereafter. A finer scan in another cool-down (inset of Fig. 2b) confirms that this behavior is indeed reproducible. The high $\zeta = 2.8$ that we observe at $B = 0 \text{ T}$ is close to values reported

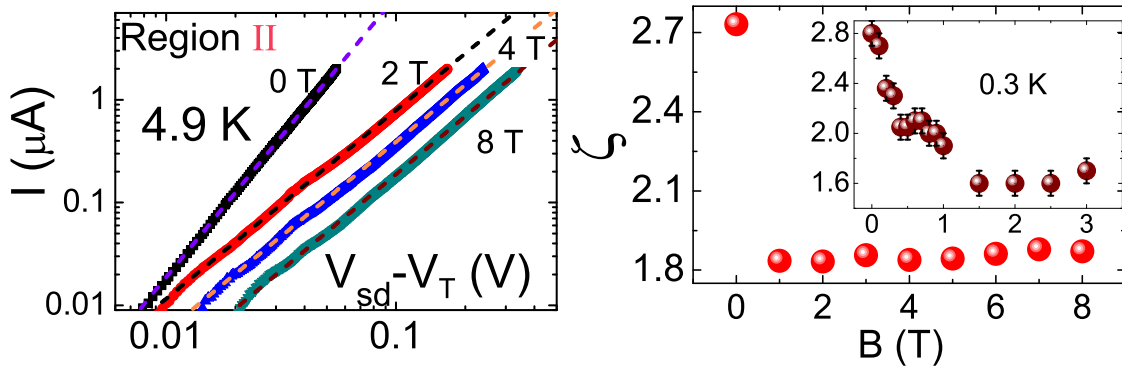


FIG. 2: (a) $I - V_{sd}$ characteristics (with threshold V_T subtracted) cast in the log-log plot for magnetic fields 0 T, 2 T, 4 T and 8 T at 4.9 K. Dashed lines represent power law fitting of the respective curve (b) Plot of ζ as a function of magnetic field B for measurements presented in (a). Inset: A finer scan of ζ vs B (at 0.3 K) for another cool-down

for array of quantum dots with structural disorder [4], whereas $\zeta \simeq 1.6$ at higher B is consistent with Middleton-Wingreen model of a capacitively coupled quantum dot array with on-site charge offset disorder [1]. The reason for this transition of ζ with B is unclear, but may be connected to redistribution of the charge inhomogeneity due to wavefunction squeezing in the puddles. Nonetheless, the $I - V_{sd}$ traces indicate that at sub-pinch-off gate voltages the 2DES is highly inhomogeneous, and may be visualised as an array of quantum dots with large structural and size disorder.

BIAS DEPENDENCE OF NLMR

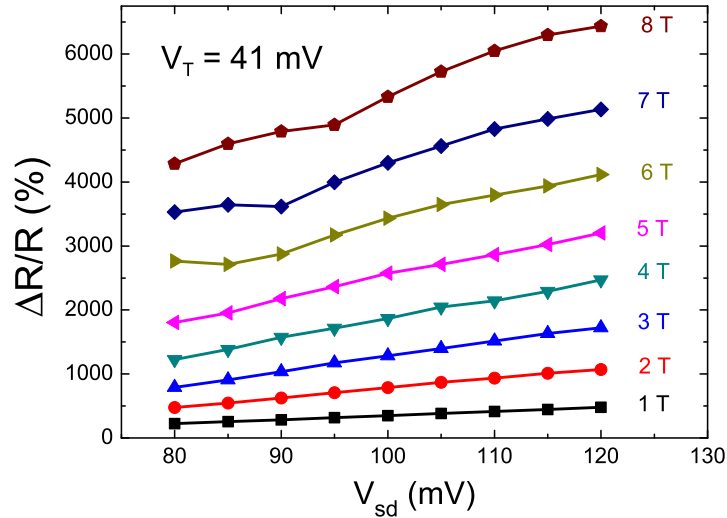


FIG. 3: $\Delta R/R$ as a function of V for magnetic fields from 1 T to 8 T at 4.9 K

The fact that ζ drops significantly from 2.8 (at $B = 0$) to 1.8 (at $B = 0$, and thereafter) implies that beyond the voltage threshold, I increases much faster when the magnetic field is zero. In other words, with increasing V_{sd} , $R(B = 0)$ drops faster than $R(B > 0)$. As a result, $\Delta R/R$ (as defined in the main text) is an increasing function of V_{sd} . Fig. 3 shows the variation of MR with V_{sd} for all the magnetic fields from 1 T to 8 T.

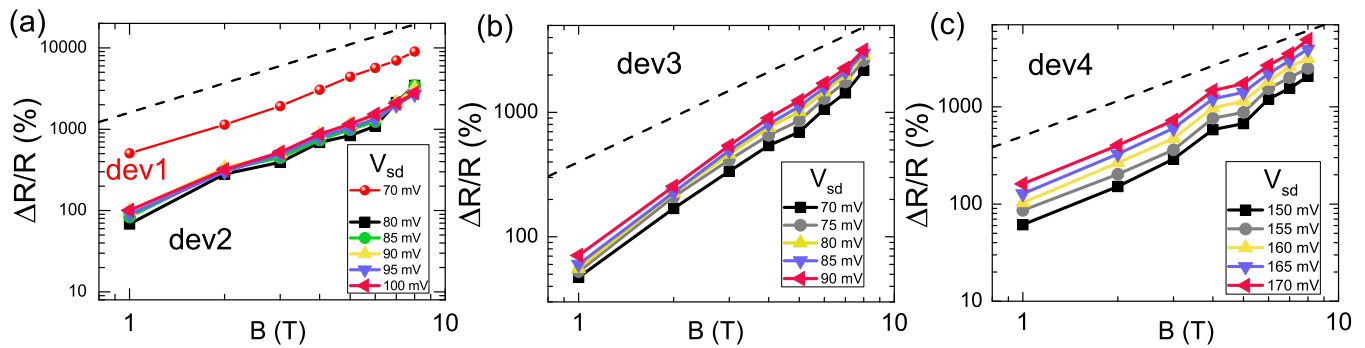


FIG. 4: (a) Comparison of linear MR of the dev1 (reported in the paper) with that of dev2 (b) dev3 (c) dev4. In all plots, the dashed line is a power law curve with exponent 1.2

LINEAR MAGNETORESISTANCE IN OTHER DEVICES

Fig. 4 presents $\Delta R/R$ (calculated in the same way as in the main text) for other devices dev2, dev3 and dev4 in another GaAs/AlGaAs heterostructure wafer. Fig. 4a compares one of the MR curves for dev1 (from Fig. 3b of the main text) with those of dev2. The form of the MR for dev2 is same as dev1 and follows a power law with exponent 1.2 (dashed line), thus exhibiting a near linear dependence. Fig. 4b and Fig. 4c show MR from two devices which show a slightly different exponent.

THEORETICAL FOUNDATION OF NLMR IN AN INHOMOGENEOUS MEDIUM

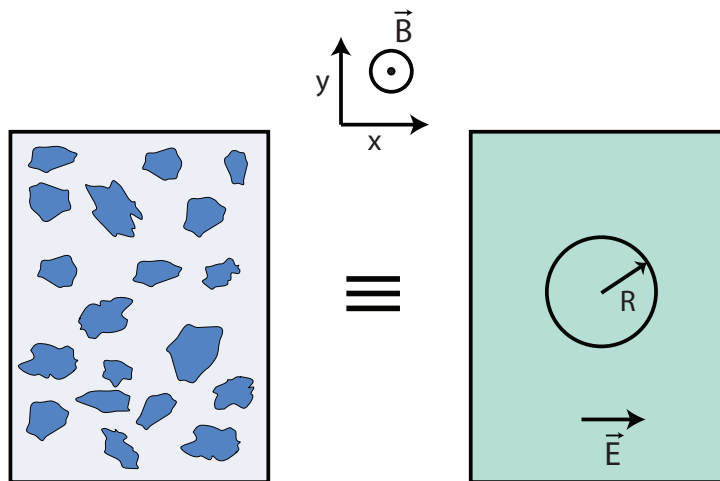


FIG. 5: Schematic describing the model used to understand the NLMR: Left: A two-dimensional conducting medium is dispersed inhomogeneously with another material. Right: An effective medium equivalent to the one on the left.

In order to understand the linear magnetoresistance in an inhomogeneous medium, we adapt the 3D magnetoresistance analysis of Stachowiak [11] (itself motivated by Herring's effective medium treatment [12]) to 2D systems. Consider a two-dimensional conducting material in the $x - y$ plane (Fig. 5) with longitudinal and Hall conductivities σ_{11} and σ_{12} respectively in presence of a magnetic field H_z in the z -direction. Suppose we make another 2D conductor by inhomogeneously dispersing this material. The local conductivity of this composite material is $\sigma = \begin{pmatrix} \sigma_{11} & \sigma_{12} \\ -\sigma_{12} & \sigma_{11} \end{pmatrix}$. We denote the corresponding effective conductivity of the composite by $\tilde{\sigma} = \begin{pmatrix} \tilde{\sigma}_{11} & \tilde{\sigma}_{12} \\ -\tilde{\sigma}_{21} & \tilde{\sigma}_{11} \end{pmatrix}$. We would like to obtain a relation between the local and effective conductivity. The measured resistivity of the sample is given by $\tilde{\rho} = \tilde{\sigma}_{11}/(\tilde{\sigma}_{11}^2 + \tilde{\sigma}_{12}^2)$.

Consider a small circular region of radius R made of the conducting material and embedded in an effective medium formed of the composite. Let there be a uniform electric field E_{0x} along the x -direction far from this disc. The resulting current \mathbf{j} everywhere satisfies the continuity equation, $\nabla \cdot \mathbf{j} = 0$. Using Ohm's law, $\mathbf{j} = \tilde{\sigma} \mathbf{E}$ etc., together with the definition $\mathbf{E} = -\nabla\psi$, where ψ is the electrostatic potential, it is easily seen that the Laplace equation $\nabla^2\psi = 0$ is satisfied. We need the solution for ψ subject to the following boundary conditions: (a) $\lim_{r \rightarrow \infty} \nabla\psi = -(E_{0x}, 0)$, (b) $\psi(r)$ is continuous at $r = R$ and (c) the normal component of the current at $r = R$, $\mathbf{j} \cdot \hat{\mathbf{r}}$, is continuous.

Solving the Laplace equation with these boundary conditions, one obtains the following solution for the potential ψ_i inside the disc:

$$\begin{aligned} \psi_i(x, y) &= C_{i1}x + D_{i1}y, \\ C_{1i} &= -\frac{3\tilde{\sigma}_{11}(2\tilde{\sigma}_{11} + \sigma_{11})E_{0x}}{(2\tilde{\sigma}_{11} + \sigma_{11})^2 + (\tilde{\sigma}_{12} - \sigma_{12})^2}, \\ D_{1i} &= \frac{3\tilde{\sigma}_{11}(\tilde{\sigma}_{12} - \sigma_{12})E_{0x}}{(2\tilde{\sigma}_{11} + \sigma_{11})^2 + (\tilde{\sigma}_{12} - \sigma_{12})^2}. \end{aligned} \quad (1)$$

Now we impose self-consistency, i.e., spatially averaging the internal field obtained above should give us the macroscopic electric fields prevailing in the effective medium. Thus imposing $\langle E_{ix} \rangle = E_{0x}$ and $\langle E_{iy} \rangle = E_{0y} = 0$ we have

$$\left\langle \frac{3\tilde{\sigma}_{11}(2\tilde{\sigma}_{11} + \sigma_{11})}{(2\tilde{\sigma}_{11} + \sigma_{11})^2 + (\tilde{\sigma}_{12} - \sigma_{12})^2} \right\rangle = 1, \quad (2)$$

$$\left\langle \frac{3\tilde{\sigma}_{11}(\tilde{\sigma}_{12} - \sigma_{12})}{(2\tilde{\sigma}_{11} + \sigma_{11})^2 + (\tilde{\sigma}_{12} - \sigma_{12})^2} \right\rangle = 0. \quad (3)$$

For classical ohmic conductors,

$$\begin{aligned} \sigma_{11} &= \frac{\sigma_0}{1 + (H_z/H_0)^2}, \\ \sigma_{12} &= \frac{\sigma_0(H_z/H_0)}{1 + (H_z/H_0)^2}, \end{aligned}$$

where $H_0^{-1} = e\tau/m$ is related to the mean free scattering time τ for the electrons in the material, and $\sigma_0 = ne^2\tau/m$ is the usual Drude conductivity. When $H_z \gg H_0$, $\sigma_{12} \sim \sigma_0(H_0/H_z) \gg \sigma_{11} \sim \sigma_0(H_0/H_z)^2$. This gives us a clue for the origin of linear magnetoresistance: in the inhomogeneous medium, the effective longitudinal conductivity takes on a bit of the local transverse conductivity.

Consider now Eq. 3. The solution is $\langle \sigma_{12} \rangle = \tilde{\sigma}_{12}$. Next in Eq. 2, consider the strong magnetic field case first where we expect $\tilde{\sigma}_{11} \gg \sigma_{11}$ on account of the admixture of σ_{12} in the effective longitudinal conductivity. This simplifies Eq. 2 to

$$\left\langle 1 - \left(\frac{\tilde{\sigma}_{12} - \sigma_{12}}{2\tilde{\sigma}_{11}} \right)^2 \right\rangle \approx \frac{2}{3},$$

which gives us

$$\tilde{\sigma}_{11} \approx \sqrt{\frac{4}{3} \langle (\tilde{\sigma}_{12} - \sigma_{12})^2 \rangle} \sim O(1/H_z). \quad (4)$$

Correspondingly, the effective longitudinal resistivity $\tilde{\rho} = \tilde{\sigma}_{11}/(\tilde{\sigma}_{11}^2 + \tilde{\sigma}_{12}^2) \sim O(H_z)$. For weak magnetic fields, the effective longitudinal conductivity will be close to σ_{11} and the magnetoresistance will go as H_z^2 .

* Electronic address: aamir@physics.iisc.ernet.in

- [1] Middleton, A. A. & Wingreen, N. S. Collective transport in arrays of small metallic dots. *Phys. Rev. Lett.* **71**, 3198–3201 (1993).
- [2] Duruöz, C. I., Clarke, R. M., Marcus, C. M. & Harris, J. S., Jr. Conduction threshold, switching, and hysteresis in quantum dot arrays. *Phys. Rev. Lett.* **74**, 3237–3240 (1995).
- [3] Rimberg, A. J., Ho, T. R. & Clarke, J. Scaling behavior in the current-voltage characteristic of one- and two-dimensional arrays of small metallic islands. *Phys. Rev. Lett.* **74**, 4714–4717 (1995).
- [4] Parthasarathy, R., Lin, X.-M. & Jaeger, H. M. Electronic transport in metal nanocrystal arrays: The effect of structural disorder on scaling behavior. *Phys. Rev. Lett.* **87**, 186807 (2001).
- [5] Reichhardt, C. & Olson Reichhardt, C. J. Charge transport transitions and scaling in disordered arrays of metallic dots. *Phys. Rev. Lett.* **90**, 046802 (2003).
- [6] Parthasarathy, R., Lin, X.-M., Elteto, K., Rosenbaum, T. F. & Jaeger, H. M. Percolating through networks of random thresholds: Finite temperature electron tunneling in metal nanocrystal arrays. *Phys. Rev. Lett.* **92**, 076801 (2004).
- [7] Goswami, S. *et al.* Transport through an electrostatically defined quantum dot lattice in a two-dimensional electron gas. *Phys. Rev. B* **85**, 075427 (2012).
- [8] Tripathi, V. & Kennett, M. P. Magnetotransport in disordered delta-doped heterostructures. *Phys. Rev. B* **74**, 195334 (2006).
- [9] Tripathi, V. & Kennett, M. P. Magnetic-field-induced coulomb blockade in small disordered delta-doped heterostructures. *Phys. Rev. B* **76**, 115321 (2007).
- [10] Neilson, D. & Hamilton, A. R. Anomalous transport in mesoscopic inhomogeneous two-dimensional electron systems at low temperature. *Phys. Rev. B* **82**, 035310 (2010).
- [11] Stachowiak, H. Effective electric conductivity tensor of polycrystalline metals in high magnetic fields. *Physica* **45**, 481 – 499 (1970).
- [12] Herring, C. Effect of random inhomogeneities on electrical and galvanomagnetic measurements. *J. Appl. Phys.* **31**, 1939–1953 (1960).